

Swift ions in radiotherapy - Treatment planning with TRiP98

M.Krämer

GSI, Planckstr. 1, D-64291 Darmstadt, Germany

Tel. +49-6159-712157, Fax +49-6159-712106

Email: M.Kraemer@gsi.de

Abstract

Since 1997 GSI operates a pilot project to treat tumours in the head and neck region with scanned beams of swift carbon ions. In order to exploit the unique physical and radiobiological properties of ion radiation, a dedicated treatment planning system (TPS) is mandatory. For this purpose the TRiP98 code package has been developed for well over a decade, in order to calculate and optimize absorbed as well as biological dose distributions for scanned ion beams. In collaboration with the DKFZ Heidelberg, the Radiological University Hospital Heidelberg and the FZ Rossendorf more than 400 patients have been planned and treated so far. This article will summarize the current capabilities of the TRiP98 TPS as well as future challenges and developments.

Keywords: Ion-beam radiotherapy, inverse treatment planning, biological dose optimization, treatment planning system.

1 Introduction

Charged particles like protons or heavier ions are becoming increasingly attractive tools for cancer radiotherapy, as can be judged from the increasing number of facilities currently in operation or being built in Germany (HIT/Heidelberg, Marburg, Kiel), Europe (PSI/Switzerland, CNAO/Italy, MedAustron/Austria, Etoile/France), and Japan (NIRS, Hyogo) [1, 2, 3]. One reason is their inverted dose profile, and their reduced or negligible lateral scattering. Moreover, charged particles offer the possibility of active dose shaping via energy variation and magnetic deflection (figure 1). This allows a much better dose conformation to arbitrary shapes of target volumes than conventional photon irradiation or ion irradiation with beam energy degraders. Consequently, all European ion-beam radiotherapy sites are or will be equipped with magnetic scanning devices.

A further advantage, in particular for heavier ions such as carbon, is their relative biological effectiveness (RBE) increasing with penetration depth. Thus the maximum of radiobiological effect is in the vicinity of - or even coincides with - the maximum of energy absorption. Moreover, different inherent radiosensitivity of different tissues can be exploited to increase the probability of killing tumour cells whilst sparing healthy tissue. This offers the opportunity of sophisticated dose optimization procedures.

Since 1997 GSI operates a successful pilot project to treat tumours in the head and neck region with scanned beams of swift carbon ions, in collaboration with the DKFZ Heidelberg, the Radiological University Hospital Heidelberg and the FZ Rossendorf. Magnetic scanning systems deliver dose distributions by superposition of several ten thousands of individual pencil beams [4, 5], usually grouped into two or more fields from different directions. This leads to rather complex radiation fields comprising particles of different

charges and very different energies. In order to exploit the unique physical and radiobiological properties of ion radiation under these conditions, a dedicated treatment planning system (TPS) is mandatory. This article will summarize the current capabilities of GSI's TRiP98 TPS as well as future challenges and developments.

2 Physical Beam Modelling

The complexity of interactions of ions heavier than protons with living matter makes it difficult - if not impossible - to provide purely experimental base data sets for treatment planning. Hence one has to rely on sufficiently accurate - and fast - model calculations to obtain base data such as depth dose distributions and charged particle spectra as a function of depth. The absorbed dose, D_{abs} , generated by an ensemble of pencil beams at locations \vec{x}_b with number of particles $\vec{N} = \{N_b\}$ at the location \vec{x} of an irradiated voxel is

$$D_{abs}(\vec{x}, \vec{N})[\text{Gy}] = 1.6 \times 10^{-8} \times \sum_b d(E_b, \vec{x}_b) \left[\frac{\text{MeV}}{\text{gcm}^{-2}} \right] G(\vec{x}, \vec{x}_b) N_b \quad (1)$$

where $d(E_b, \vec{x}_b)$ is the planar-integrated dose per incident ion of primary energy E_b in pencil beam b with number of particles N_b , and

$$G(\vec{x}, \vec{x}_b) = \frac{1}{2\pi\sigma_b^2[\text{mm}^2]} \exp\left(-\frac{1}{2} \frac{r^2}{\sigma_b^2}\right) \quad (2)$$

is the beam profile at lateral distance $r^2 = |\vec{x} - \vec{x}_b|^2$. G can also be modified by adding a second Gaussian to account for lateral scattering effects. We use a numerical home-grown transport code [6, 7] integrated into TRiP98, which includes the most important basic interactions, i.e. electronic energy loss, energy loss straggling, and nuclear reaction/fragmentation, to calculate d . Lateral scattering processes such as the angular distribution after nuclear interactions and subsequent multiple Coulomb scattering can be

taken into account and are incorporated in G . For homogeneous media (water), these calculations can be performed without resorting to Monte Carlo methods. The resulting depth dose distributions, i.e. the quantities $d \times G$, as well as the associated charged particle energy spectra, are precalculated for a set of energies E_b and stored as a base dataset. Thus equation 1 can be evaluated within a few minutes or seconds even for complex treatment plans. Inhomogeneities can be handled via experimental calibration tables to convert the Hounsfield units supplied by a computer tomographic (CT) image to water-equivalent path lengths [8]. The largest - and most critical - impact of inhomogeneities is on ion range, which has to be calculated with an accuracy of 0.5 mm, corresponding to half the size of a voxel of a CT image.

3 Radiobiological Effects

For all ions heavier than protons the inclusion of radiobiological effects into regular treatment planning is indispensable. Observables like cell survival probabilities, biological effective dose and RBE depend on a multitude of different parameters [9]. Densely ionizing radiation, i.e. high- Z low-energy particles are expected to cause the highest biological effect. Clearly, RBE depends also on the type of tissue under consideration. The radiosensitivity of a particular cell type is dominated by the efficiency of its repair mechanism. Repair-deficient mutants of an otherwise repair-efficient cell line may exhibit an entirely different dose response, although the radiation physics is almost the same (Figure 2), making ab-initio modelling almost impossible. For the purposes of treatment planning, the dependency on absorbed dose - or particle fluence - is extremely important, because many different dose levels will occur, from the full target dose of several Gy per fraction down to a few percent of the target dose at the edges of the irradiated volume. Dose dependency

follows from the definition of RBE via dose-effect curves (Figure 3), which shows that RBE increases with decreasing dose, up to a maximum RBE_α for doses approaching zero. Because dose-effect curves are linear-quadratic for a particle of given charge and energy, simple linear addition of biological dose values is not possible. This nonlinearity is one of the challenges for treatment planning involving complex radiation fields in three or even four dimensions, i.e. including motion of the irradiated organs.

Since ab-initio calculations of biological effects are so far neither reliable nor computationally feasible, we use the versatile Local Effect Model [10, 11] in its high-speed implementation [12]. With the algorithms specified by the LEM model, biological effects of complex mixed radiation fields can be calculated efficiently and correctly on a voxel-by-voxel basis from the local particle distribution [13, 12]. The biological dose distribution then is

$$D_{bio}(\vec{x}, \vec{N}) = D_{abs}(\vec{x}, \vec{N}) \times \text{RBE}(\vec{x}, \vec{N}). \quad (3)$$

Efficient and voxel-based calculations are especially important if not only forward dose calculation is desired but also dose optimization by inverse planning with the necessity to recalculate the dose distribution many times for different sets of \vec{N} .

4 Biological Dose Optimization

The main task of treatment planning for scanning systems actually is the determination of the particle numbers \vec{N} in the individual pencil beams in order to obtain the prescribed target dose, D_P , under the constraint that excessive dose values in organs at risk (OAR) should be avoided. This can be formulated as a least-squares minimization problem, which

reads in simplified form (omitting weight factors):

$$\chi^2 = \sum_{\vec{x}_{target}} (D_P(\vec{x}) - D_A(\vec{x}))^2 + \sum_{\vec{x}_{OAR}} (D_P(\vec{x}) - D_A(\vec{x}))^2 \times \theta(D_A(\vec{x}) - D_{OAR}(\vec{x})) = min. \quad (4)$$

where $D_A(\vec{x})$ is the actual dose distribution calculated according to Equation 3, $D_{OAR}(\vec{x})$ is the maximum allowed biological dose in the OAR, and θ the Heaviside function, whose purpose is to impose a penalty if $D_{OAR}(\vec{x})$ is exceeded, but to do nothing if the actual dose is below that limit. The sum runs over all voxels in the target and the OAR, respectively. The free parameters, \vec{N} , to be determined are implicitly included in $D_A(\vec{x})$ via Equations 3 and 1. The solution of Equation 4 is not trivial due to the nonlinear dependence on \vec{N} and the constraint term, but can be achieved by appropriate iterative algorithms. This may take between half an hour and up to several hours on current computer hardware, depending on the size of the involved volume. Up to 100000 voxels and up to 70000 different pencil beams may be required for a single treatment plan. Figure 4 shows a resulting biological dose distribution.

5 Verification

Absorbed dose distributions are usually verified experimentally by means of calibrated ionization chambers (IC) [14]. Under certain circumstances, however, solid state detectors like TL dosimeters [15] or radiographic films [16] are advantageous. In particular under presence of motion [17] film dosimetry still is a valuable verification tool. Unlike ICs, however, the dose response of solid state detectors depends explicitly on the charge and energy of the particles which constitute the radiation field, for similar reasons as the response of biological systems. Hence charge- and energy-dependent efficiency tables must be established [18, 19] and only forward calculations, i.e. prediction of dosimeter response

under the assumption of a known field composition, can be verified by such detection devices. This method is supported by built-in procedures in TRiP98.

The ultimate goal of radiotherapy is to achieve biological effect rather than just delivering absorbed dose distribution. Thus it is a good idea to be able to verify the calculations by means of biological dosimetry, i.e. by measuring cell survival distributions after irradiation. For this purpose a so-called Bio-Phantom (Figure 5) was developed and is regularly used to verify typical treatment situations under patient-like conditions. Figure 6 shows the biological verification of a complex irradiation plan, thereby testing the whole planning chain including the computational models as well as the irradiation device.

6 Conclusion and Outlook

TRiP98 is a TPS for scanned ion beams which can handle calculation and optimization of absorbed and biological effective dose distributions of complex ion radiation fields in three dimensions. It supports various verification methods, including biological dosimetry. It is in clinical use since 1997. More than 400 patients have been successfully planned and treated so far [20].

One of the main future tasks is treatment planning in four dimensions, to support irradiation under presence of motion of both, the scanned beam as well as the irradiated organs [21]. The necessary enhancements to include biological effects are currently being built into TRiP98. First results from experimental verifications are very encouraging.

Another line of development is the extension of TRiP98 to other light ion beams, such as helium and oxygen, and possibly lithium. Physical as well as radiobiological properties predicted by the current models have to be verified experimentally. Inclusion of the respective base data sets into the TPS will allow realistic studies whether significant

advantages exist for specific tumour types and locations.

Further efforts are devoted to the improvement of the biological model (LEM), in particular by investigating the local dose deposition in the ion track core [24]. This requires more experimental and theoretical knowledge on creation and transport of δ -electrons in the energy region below some hundred eV [25].

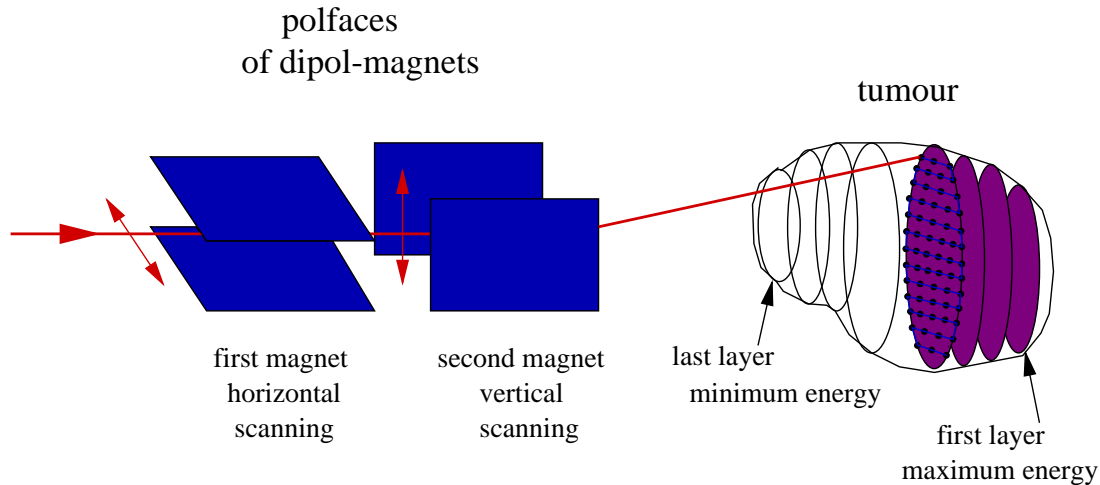
References

- [1] Amaldi U., Kraft G. AAPPS Bulletin, 18(1) (2008) 19-23.
- [2] PTCOG, <http://ptcog.web.psi.ch/>, retrieved Jul-2008.
- [3] J.Sisterson, Particles Newsletter, 35 (2005).
- [4] E. Pedroni et al, Med. Phys. 22 (1993) 37-53.
- [5] Th. Haberer, W. Becher, D. Schardt, G. Kraft, Nucl. Instrum. Meth. A330 (1993) 296-305.
- [6] M. Krämer, O. Jäkel, Th. Haberer, G. Kraft, D. Schardt, U. Weber, Phys. Med. Biol., 45(11) (2000) 3299-3317.
- [7] Th. Haberer, Entwicklung eines magnetischen Strahlführungssystems zur tumorkonformen Strahlentherapie mit schweren geladenen Teilchen, GSI-report 94-09 (in German).
- [8] E. Rietzel, D. Schardt, Th. Haberer, Rad. Oncology, 2 (2007) 14.
- [9] M. Krämer, W.K. Weyrather, M. Scholz M, Technol. Cancer Res. Treat., 2(5) (2003) 427-436.

- [10] M. Scholz, A.M. Kellerer, W. Kraft-Weyrather, G. Kraft, *Rad. Environ. Biophysics* 36 (1997) 59-66.
- [11] T. Elsässer, M. Scholz, *Rad. Res.*, 167 (2007) 319-329.
- [12] M. Krämer, M. Scholz, *Phys. Med. Biol.* 51 (2006) 1959-1970.
- [13] M. Krämer, M. Scholz, *Phys. Med. Biol.*, 45(11) (2000) 3319-3330.
- [14] C.P. Karger, O. Jäkel, G.H. Hartmann, P. Heeg, *Med. Phys.* 26(10) (1999) 2125-2132.
- [15] O. Geiß, M. Krämer, G. Kraft, *Nucl. Instr. and Meth. B* 146 (1998) 541-544.
- [16] B. Spielberger, M. Krämer and G. Kraft *Phys. Med. Biol.* 48/4, (2003) 497-505.
- [17] C. Bert, N. Saito, A. Schmidt, N. Chaudhri, D. Schardt, E. Rietzel, *Med. Phys.* 34(12) (2007) 4768-4771.
- [18] O. Geiß, M. Krämer, G. Kraft, *Nucl. Instr. and Meth. B* 142 (1999) 592.
- [19] B. Spielberger, M. Scholz, M. Krämer and G. Kraft *Phys. Med. Biol.* 47/22 (2002) 4107-4120.
- [20] D. Schulz-Ertner, C.P. Karger, A. Feuerhake, A. Nikoghosyan, S.E. Combs, O. Jäkel, L. Edler, M. Scholz, J. Debus, *Int. J. Radiat. Oncol. Biol. Phys.*, 68(2) (2007) 449-457.
- [21] Ch. Bert, E. Rietzel, *Rad. Oncology*, 2 (2007) 24.
- [22] W.K. Weyrather, S. Ritter, M. Scholz, G. Kraft, *Int. J. Radiat. Biol.*, 75 (11) (1999) 1357-1364.
- [23] M. Krämer, J.F. Wang, W.K. Weyrather, *Phys. Med. Biol.* 48/14 (2003) 2063-2070.

- [24] Th. Elsässer, R. Cunrath, M. Krämer, M. Scholz, *New J. Phys. Focus on Heavy Ions in Biophysics and Medical Physics*, 10 (2008) 075005
- [25] N. Lineva, C. Kozhuharov, S. Hagmann, M. Krämer, G. Kraft, *Nucl. Instr. and Meth.*, this issue.

Figure 1: Schematic view of the GSI magnetic scanning system



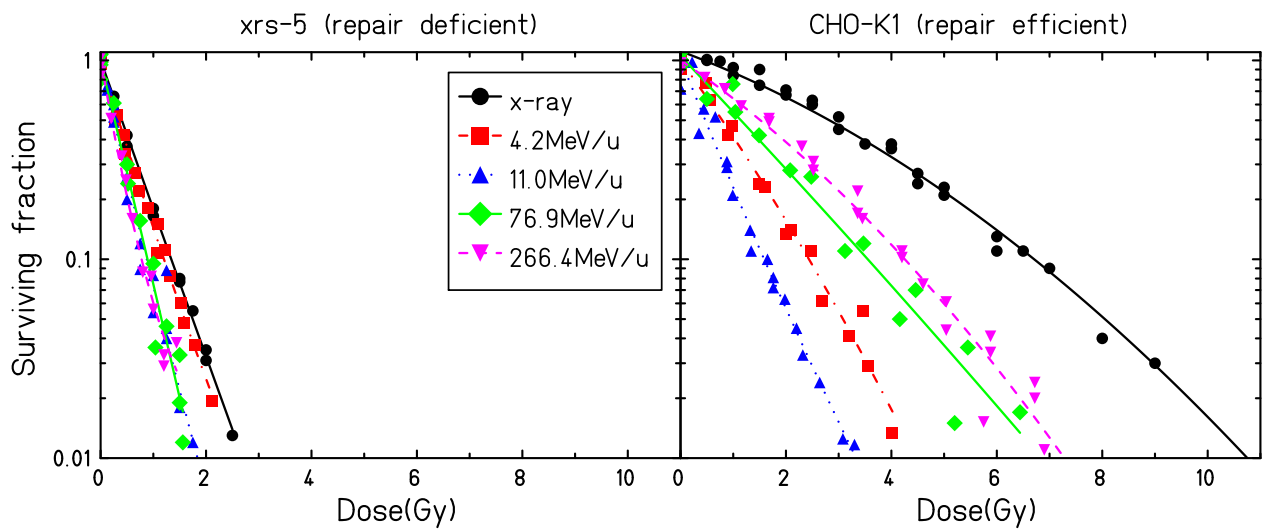


Figure 2: Comparison of the vastly different dose responses of repair deficient (xrs5) and repair efficient (CHO-K1) mutations of the same cell line [22]. ^{12}C ions with various energies (as indicated in the legend) have been used, as well as X-rays for reference.

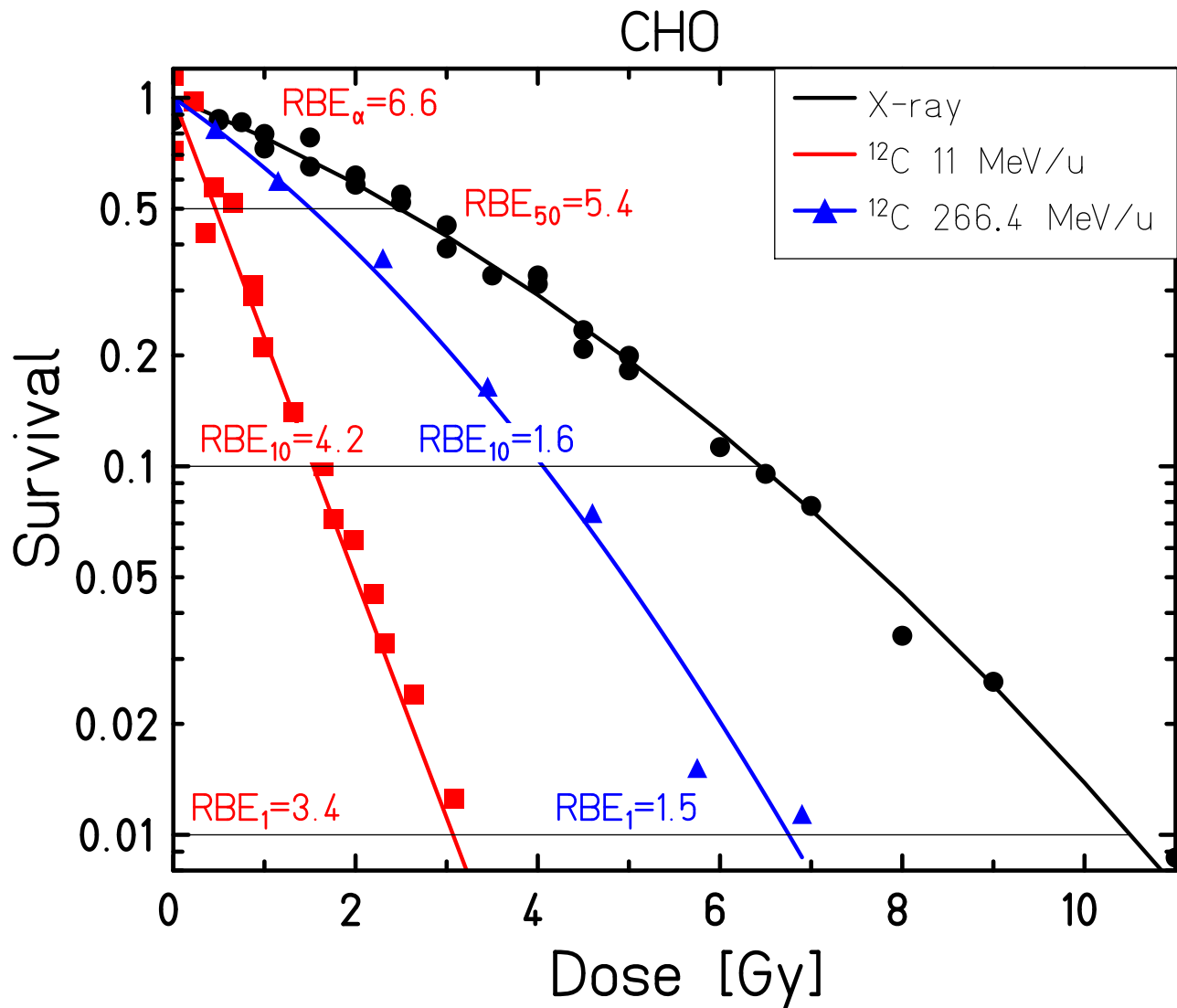


Figure 3: Definition of RBE as the ratio of the photon dose to the absorbed ion dose leading to the same biological effect. Different RBE values are obtained for different survival levels, hence RBE is dose dependent. Symbols are experimental data, curves represent linear-quadratic fit curves.

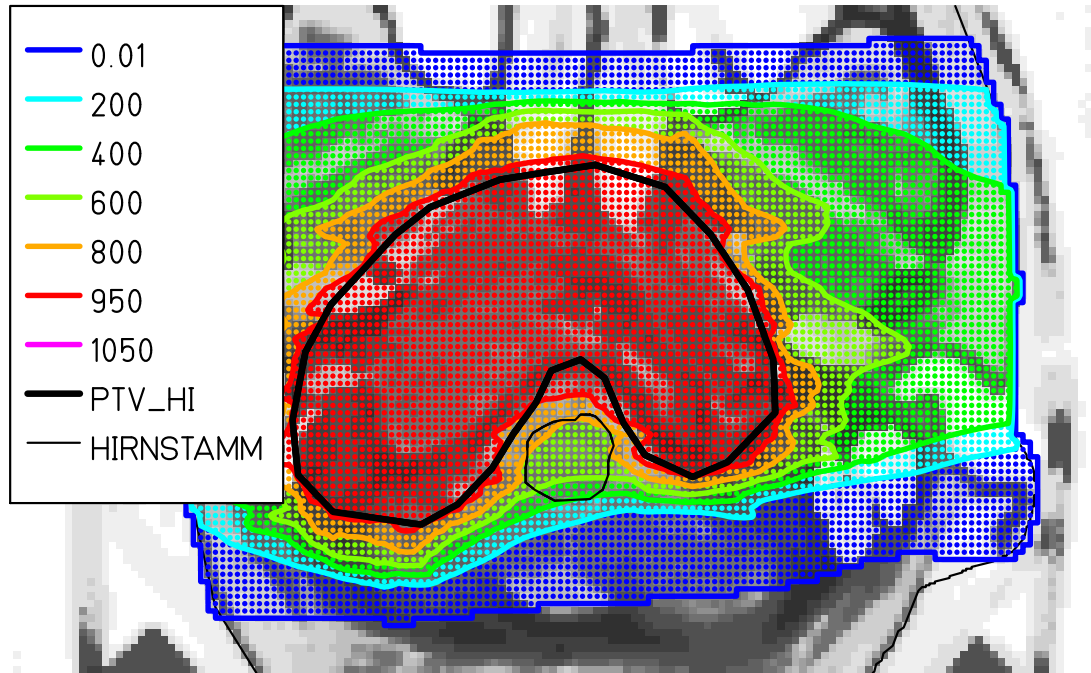


Figure 4: Optimized biological dose distribution generated by two opposing fields entering from the left and right hand side, respectively. The central two-dimensional slice of the CT image is shown with the biological dose distribution overlaid. The colours correspond to the dose levels listed in the insert, given in permille of the prescribed biological dose in the tumour volume, which was 3 Gy. Although the brain tumour wraps around the critical organ (brain stem), the latter could largely be spared.

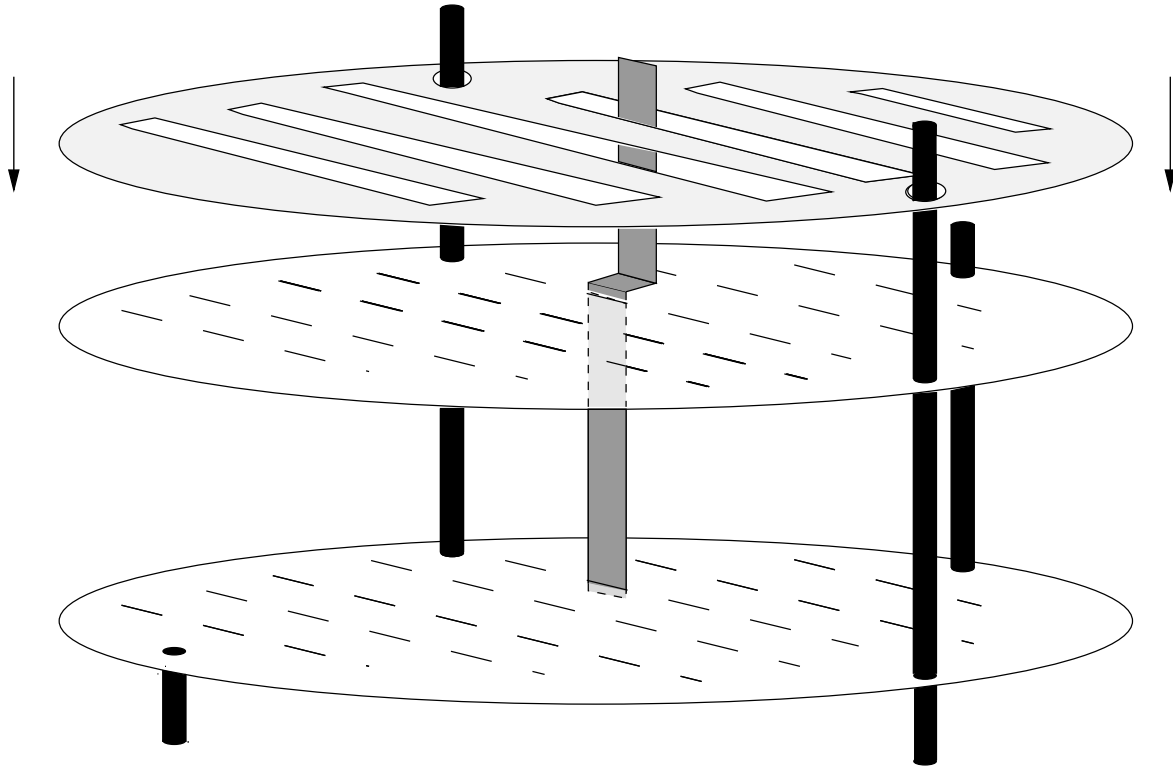


Figure 5: Schematic view of the Bio-Phantom. Cell covered plastic strips are inserted into the slits, thereby defining a two-dimensional measuring grid. The whole arrangement is inserted into a vessel with culture medium prior to irradiation.

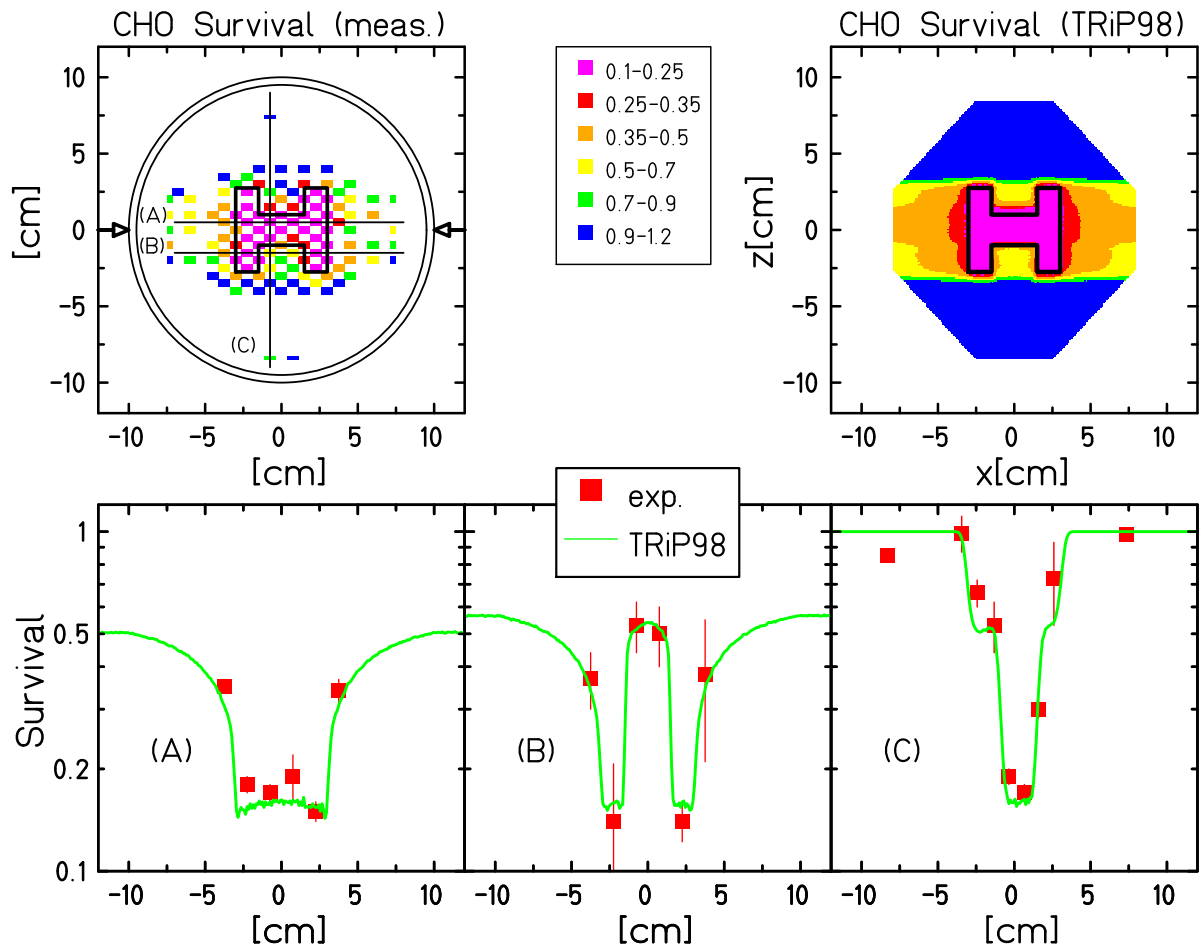


Figure 6: Two-dimensional biological verification of a complex radiation field with CHO cells [23]. The H-like target volume is irradiated with two partial fields from the left and the right hand side. The measured cell survival probability (upper left graph) compares well with the TPS predictions (upper right graph). The one-dimensional cuts (lower panel) allow a more quantitative comparison (symbols: experiment, curves: TRiP98 calculation).